Available online at www.sciencedirect.com
ScienceDirect
Journal of the European Ceramic Society 31 (2011) 225–229
www.elsevier.com/locate/jeurceramsoc

Technical note

Polymer template fabrication of porous hydroxyapatite scaffolds with interconnected spherical pores

K. Zhao *, Y.F. Tang, Y.S. Qin, D.F. Luo

Department of Materials Science and Engineering, Xi'an University of Technology, 5 South Jinhua Road, Xi'an, Shaanxi 710048, PR China

Received 27 May 2010; received in revised form 29 August 2010; accepted 7 September 2010

Abstract

Porous hydroxyapatite (HA) scaffolds with interconnected spherical pores were fabricated by slip casting using a polymer template. Templates were produced using polymer beads, NaCl, and adhesive (N100). Effects of the preparation process on the pore structures and mechanical properties of the porous HA scaffolds were investigated. Pore interconnectivity was improved by adding NaCl particles with appropriate diameters to the polymer template. The size of the adhesive area could be controlled by adjusting the concentration of N100. The pore size could be controlled between 200 ± 42 and 400 ± 81 μm, and the porosity between 50.2 and 73.1%, by changing the size of the polymer beads and the volume of the NaCl particles. The compressive strength decreased as the porosity or pore size increased.
© 2010 Elsevier Ltd. All rights reserved.

Keywords: Slip casting; Porosity; Mechanical properties; Hydroxyapatite; Biomedical applications

1. Introduction

Porous hydroxyapatite (HA) scaffolds have attracted considerable attention due to their high osteoconductivity and bioactivity for hard tissue applications.[1–3] Studies have focused on porous scaffolds with spherical pores, due to the fact that their pore configuration can increase stress tolerance. The properties of the pores in these scaffolds, such as size, porosity and geometry, and mechanical properties are the key governing factors in HA application.[4,5] In recent years, meaningful progress has been made with porous HA scaffolds.[6–9] Improvements in mechanical strength[10–12] and control of pore structures[13–15] have been reported. Among the reported approaches, polymer bead stacking templates are one of the most promising methods for fabricating spherical porous ceramic scaffolds, and the considerable progress was made in precise control of scaffold porosity and internal pore structures parameters.[16,17] Extensive research on improvement of the compressive strength of porous HA scaffold has shown that reduced porosity can significantly improve the mechanical properties of porous scaffolds with the same pore size.[18–20] However, pore connectivity is reduced when the number of closed pores increases (i.e., porosity reduces).

In this work, we proposed a new method to fabricate porous HA scaffolds with interconnected spherical pores by using a polymer template. The strategy for polymer template production involved: (i) distribution of NaCl particles in the gaps between polymer beads so that the beads did not touch each other; (ii) formation of an adhesive area among the polymer beads by adding adhesive (N100); and (iii) removal of NaCl particles by washing for 30 min in deionized water, and then drying. Effects of the preparation process on the pore structures and mechanical properties of the porous HA scaffolds were investigated.

2. Experimental procedure

Commercially available HA powder (Fluka Co., UK) with a size of 0.5–1.0 μm was taken as the starting material. Poly(styrene-co-divinylbenzene) beads (Sigma–Aldrich Chemical Co. Inc.) with sizes of 300 ± 50 μm, 450 ± 50 μm and 600 ± 50 μm were used as polymer templates. N100 (ethylbenzene containing 10% polystyrene and other compounds) was used as an adhesive. NaCl particles (analytical reagent grade, 170–500 μm, Xi'an Chemical Reagent, China) were served as a filling agent for controlling the connectivity of the polymer template. In addition, deionized water, anhydrous ethanol

* Corresponding author. Tel.: +86 29 82312601; fax: +86 29 82312922.
E-mail address: kzhao.xaut@gmail.com (K. Zhao).

0955-2219/$ – see front matter © 2010 Elsevier Ltd. All rights reserved.
doi:10.1016/j.jeurceramsoc.2010.09.007

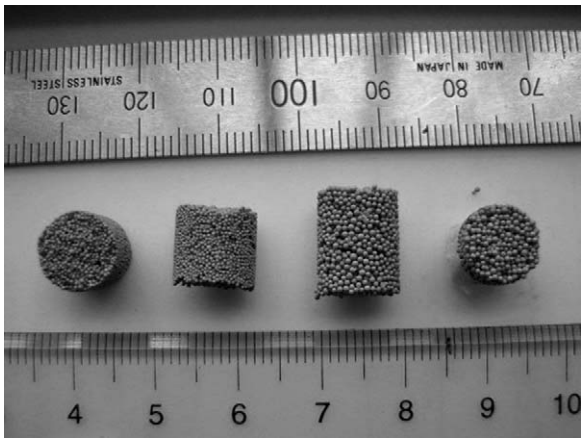

Fig. 1. Photographs of polymer templates.

(analytical reagent grade, Xi'an Chemical Reagent, China), and polyvinyl butyral (PVB, Xi'an Chemical Reagent, China) were used as rinse agent, solvent, and binder, respectively.

NaCl particles and polymer beads in different diameter ratios (0.45, 0.5, 0.6 and 0.7) were mixed by drum material mixing (250r/min) without balls and medium and placed in polyethylene cylinders (diameter 10 mm). Liquid N100 adhesive was filled from the top of polyethylene cylinder, went through whole space and out-flowed from the bottom, so that it could adhere in gaps between the polymer beads to bond them after dried. The dried polymer template was washed for 30 min in deionized water to remove the NaCl, and then dried again. The polymer template is shown in Fig. 1. HA powder (10 g) was mixed with 20 mL of anhydrous ethanol and 1% PVB, and placed in a ball-mill for approximately 4 h to form a slurry. The slurry was poured into the polymer template and dried for 8 h at 80 °C. The sample was then sintered at 1250 °C for 2 h, the heating rate and the cooling rate were 5 °C/min. During sintering, the organic material decomposed at 400–600 °C, and the HA ceramic underwent densification at 1100–1250 °C.

The morphologies of the polymer templates and porous HA scaffolds were observed by scanning electron microscopy (SEM, model JSM-6700F, JEOL, Japan). The total and open porosity of the scaffolds were tested using Archimedes' method. The compressive strength of each scaffold was measured using a computer servo control material testing machine (HT-2402-100KN, Hungta, Taiwan) at a punch rate of 0.2 mm/min. More than five specimens were tested to get the averaged results for each condition. The size of the adhesive area was determined by measuring each adhesive area in SEM images of five specimens of the polymer template using the digital image tool (Commercial software, version 2.0, Digital Liquid Ltd.), and the precision obtained was estimated to be 5%.

3. Results and discussion

Polymer templates were constructed by using polymer beads with pore diameters of 300 ± 50 μm and different N100 adhesive concentrations (30, 50, and 70%). SEM images (Figs. 2(a) and (b)) were obtained for the adhesive area between two polymer beads in the templates produced using 30 and 70% N100. The capability of N100 to adhere the polymer beads to each other increased with increasing N100 concentration. Accordingly, the size of the adhesive area between the polymer beads increased. These results suggest the neck size of interconnected pores in a HA scaffold produced using a polymer template could be controlled by changing the adhesive area between the polymer beads. The adhesive areas were measured for templates produced with different concentrations of N100 (Table 1). In addition to the influence of N100 concentration, increasing the size of the polymer beads also increased the size of the adhesive area (Table 1). Fig. 3 shows SEM images of HA scaffolds made by slip casting from the polymer templates produced with different N100 adhesive concentrations. As hypothesized, the neck size of the porous HA scaffold was determined by the size of the adhesive area between beads in the polymer template.

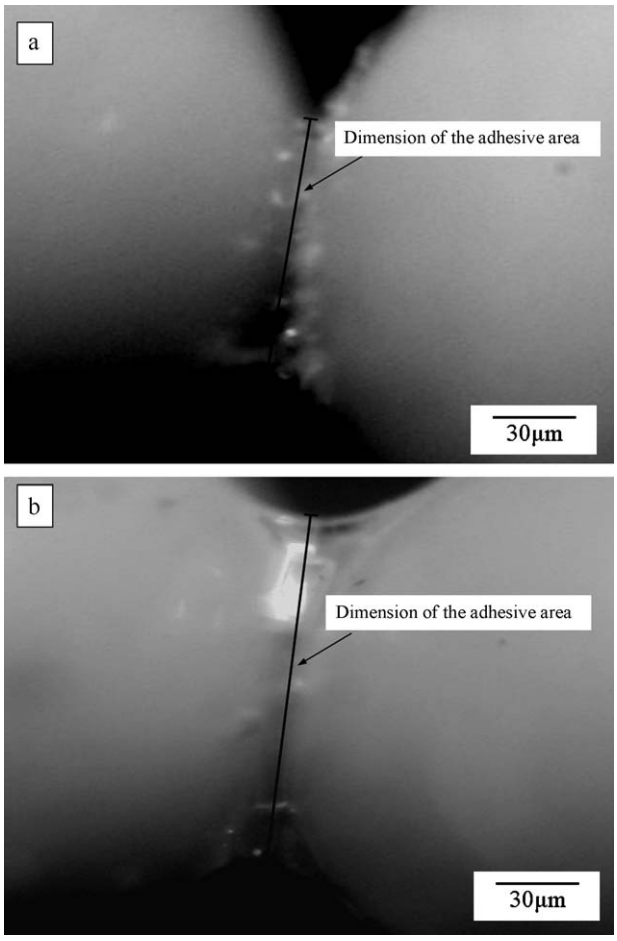

Fig. 2. Scanning electron microscopy micrographs of polymer templates produced with different adhesive concentrations: (a) the adhesive area formed when the mass fraction of N100 was 30%, and (b) the adhesive area formed when the mass fraction of N100 was 70%.

The size of pores in the HA scaffolds could be controlled primarily by varying the size of polymer beads and the sintering shrinkage, because pores were formed as a result of decomposition of these beads. The shrinkage was defined as the ratio of the diameter of the pores in porous HA scaffolds to that of polymer beads in the polymer template and are found in the range of

Table 1
The relationship between the N100 concentration and the size of the adhesive area between polymer beads in the polymer templates.

N100 concentration (wt%)	Dimension of adhesive area (μm)		
	Bead size of 300 ± 50 μm	Bead size of 450 ± 50 μm	Bead size of 600 ± 50 μm
30	55.9 ± 2.3	104.3 ± 3.9	212.6 ± 5.2
50	101.2 ± 3.8	176.2 ± 4.2	354.8 ± 6.3
70	128.6 ± 4.9	220.6 ± 5.4	442.5 ± 7.1

wt%—weight percentage.

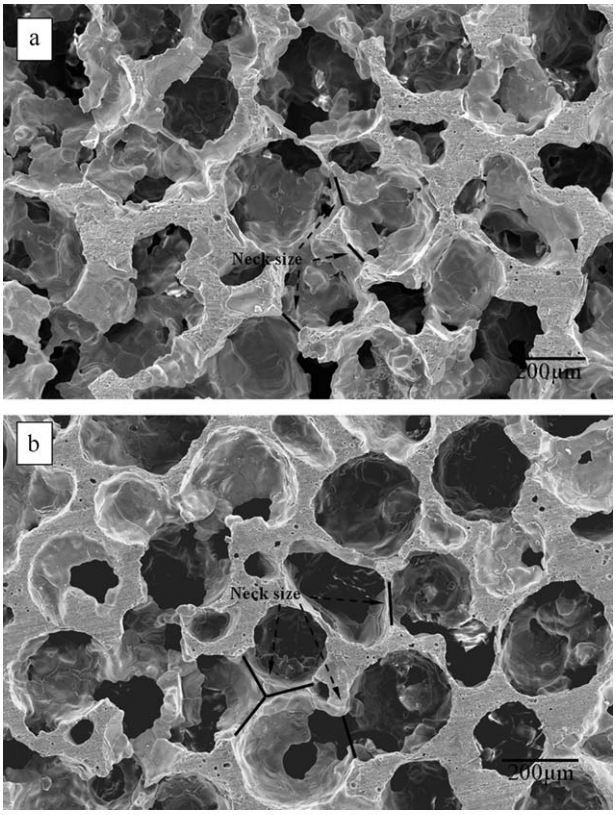

Fig. 3. Scanning electron microscopy micrographs of HA scaffolds illustrating the effect of adhesive concentration on neck size of interconnected pores: (a) formed when the mass fraction of N100 was 30%, and (b) formed when the mass fraction of N100 was 70%.

31.7–33.5% (Table 2). The key factor for maintaining interconnectivity of pores is the selection of appropriate diameter ratios of NaCl particles to polymer beads ($R_{NaCl}/R_{polymer}$). If the diameter ratio is too small, NaCl particles will not be large enough to effectively space the polymer beads. If the ratio is too large, the polymer beads will be too far apart and the adhesive will not be able to bind them together. Assuming that NaCl consists of rigid spheres, the packing of NaCl particles and polymer beads with octahedral and tetrahedral interstices can be schematically represented in Fig. 4.

Here, when the NaCl particle located in an octahedral interstice among polymer beads:

$$\frac{R_{NaCl}}{R_{polymer}} = \sqrt{2} - 1 \approx 0.414 \quad (1)$$

and, when the NaCl particle is located in a tetrahedral interstice among polymer beads:

$$\frac{R_{NaCl}}{R_{polymer}} = \frac{\sqrt{6}}{2} - 1 \approx 0.225 \quad (2)$$

Eqs. (1) and (2) indicate that when $R_{NaCl}/R_{polymer} > 0.414$, NaCl can act as a filler. Consequently, in our experiments we used $R_{NaCl}/R_{polymer}$ ratios of 0.45, 0.5, 0.6, and 0.7 to investigate the optimal ratio. Table 3 shows the total porosities and open porosities of scaffolds prepared with the different $R_{NaCl}/R_{polymer}$ ratios. These results show that the $R_{NaCl}/R_{polymer}$ ratio affects the open porosity, but not the total porosity. With an $R_{NaCl}/R_{polymer}$ ratio between 0.45 and 0.6, the changes in open porosity were within about 1%. This demonstrates good interconnectivity of the HA scaffold. When the $R_{NaCl}/R_{polymer}$ ratio was increased up to 0.7, there was a large decrease in open porosity (to 48.12%). With a larger R_{NaCl}, polymer beads could not form adhesive areas and this resulted in some closed pores and a decrease

Table 2
The relationship between the sizes of the polymer beads and the pore size of the porous HA scaffolds.

Dimension of polymer beads (μm)	Pore size of HA scaffold (μm)	Shrinkage (%)
300 ± 50	199.8 ± 42	33.4 ± 2.6
450 ± 50	307.4 ± 65	31.7 ± 6.2
600 ± 50	399.0 ± 81	33.5 ± 7.3

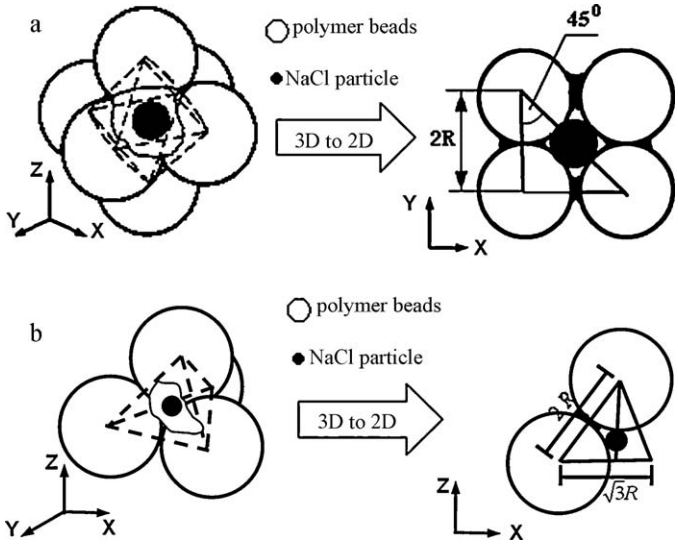

Fig. 4. A schematic representation of mixing of NaCl particles and polymer beads with: (a) octahedral interstices, and (b) tetrahedral interstices.

Table 3
The total porosity and the open porosity of the HA scaffolds prepared with different $R_{NaCl}/R_{polymer}$ ratios.

$R_{NaCl}/R_{polymer}$	Total porosity (%)	Open porosity (%)
0.45	67.6 ± 1.0	66.87 ± 0.04
0.5	67.2 ± 1.2	65.62 ± 0.27
0.6	68.0 ± 0.7	64.89 ± 0.44
0.7	66.8 ± 1.4	48.12 ± 1.20

R_{NaCl}, the diameter of NaCl particles; $R_{polymer}$, the diameter of polymer beads.

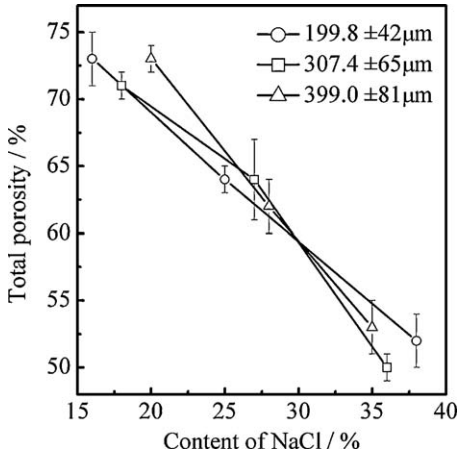

Fig. 5. The relationship between the content of NaCl and the total porosity of porous HA scaffolds.

in interconnectivity. Thus, $R_{NaCl}/R_{polymer}$ ratios between 0.45 and 0.6 effectively maintain good interconnectivity. Since the $R_{NaCl}/R_{polymer}$ ratio had minor effect on the total porosity, an $R_{NaCl}/R_{polymer}$ ratio of 0.5 was used.

Fig. 5 shows the relationship between the NaCl content and total porosity. The total porosity of the samples decreased with increasing NaCl content. This is related to the method of HA scaffold formation, in which the spaces that were previously occupied by NaCl particles in the polymer templates were filled with HA slurry in the slip casting process after the NaCl particles were washed off. The relationship between compressive strength and total porosity for porous HA scaffolds with different pore sizes was also determined. The compressive strength of the porous HA scaffolds decreased markedly as the porosity or pore size increased (Fig. 6). Because the compressive strength of porous ceramics have greater dependence on the cell wall strength and on its own density,[21] and the effective fracture area for absorbing load and resistance to deformation decreased as the porosity or pore size of scaffold increased. When the pore size was 199.8 μm and the porosity was 61%, the maximum compressive strength reached 7.5 MPa.

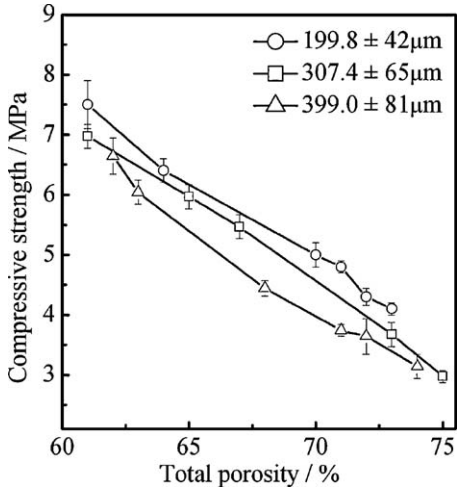

Fig. 6. The relationship between the compressive strength and the total porosity of porous HA scaffolds for different pore sizes.

4. Summary

Porous HA scaffolds with interconnected pores were produced using a polymer template from polymer beads, NaCl, and adhesive (N100). Altering the concentration of N100 used in the template production allowed control of the size of the adhesive area. The size of pores in the HA scaffolds could be manipulated between 200 ± 42 and 400 ± 81 μm and the porosity between 50.2 and 73.1% by controlling the polymer bead diameters to 300 ± 50 to 600 ± 50 μm, and the volume of the NaCl particles. The interconnectivity of the porous HA scaffolds was improved when diameter ratios $R_{NaCl}/R_{polymer}$ in the range of 0.45–0.6 were used. The maximum compressive strength was 7.5 MPa when the porosity was 61% and the pore size was approximately 199.8 μm, it decreased markedly as the porosity or pore size increased.

Acknowledgements

The authors would like to thank the support from the National Natural Science Foundation of China (No. 50872110), the Shaanxi Provincial Project of Special Foundation of Key Disciplines (No. [2008]171) and the Foundation of Excellent Doctoral Dissertation of Xi'an University of Technology.

References

1. Walsh WR, Chapman-Sheath PJ, Cain S, Debes J, Bruce WJM, Svehla MJ, et al. A resorbable porous ceramic composite bone graft substitute in a rabbit metaphyseal defect model. *J Orthopaedic Res* 2003;**21**:655–61.
2. Hasegawa S, Tamura J, Neo M, Goto K, Shikinami Y, Saito M, et al. In vivo evaluation of a porous hydroxyapatite/poly-DL-lactide composite for use as a bone substitute. *J Bio Mater Res Part A* 2005;**75**:567–79.
3. Sepulveda P, Ortega FS, Innocentini MDM, Pandolfelli VC. Properties of highly porous hydroxyapatite obtained by the gelcasting of foams. *J Am Ceram Soc* 2000;**83**:3021–4.
4. Burg KJL, Porter S, Kellam JF. Biomaterial developments for bone tissue engineering. *Biomaterials* 2000;**21**:47–59.
5. Takafumi Y, Hajime O. Human marrow cell-derived cultured bone in porous ceramics. *Bio-Med Mater Eng* 1998;**8**:11–20.
6. He F, Liu CS. Preparation of porous glass-ceramic with controlled pore size and porosity by adding porosifier. *J Inorg Mater* 2004;**19**:1267–76.
7. Nakahira A, Murakami T, Onoki T, Hashida T, Hosoi K. Fabrication of porous hydroxyapatite using hydrothermal hot pressing and post-sintering. *J Am Ceram Soc* 2005;**88**:1334–6.
8. Ramay HR, Zhang MQ. Preparation of porous hydroxyapatite scaffolds by combination of the gel-casting and polymer sponge methods. *Biomaterials* 2003;**24**:3293–302.

9. Sopyan I, Kaur J. Preparation and characterization of porous hydroxyapatite through polymeric sponge method. *Ceram Int* 2009;**35**:3161–8.
10. He QJ, Huang ZL. Controlled growth and kinetics of porous hydroxyapatite spheres by a template-directed method. *J Cryst Growth* 2007;**300**:460–6.
11. Engin NO, Tas AC. Manufacture of macroporous calcium hydroxyapatite bioceramics. *J Eur Ceram Soc* 1999;**19**:2569–72.
12. Saiz E, Gremillard L, Menendez G, Miranda P, Gryn K, Tomsia AP. Preparation of porous hydroxyapatite scaffolds. *Mater Sci Eng C* 2007;**27**:546–50.
13. Real RPD, Wolke JGC, Vallet-Regí M, Jansen JA. A new method to produce macrospores in calcium phosphate cements. *Biomaterials* 2002;**23**:3673–80.
14. Chang BS, Lee CK, Hong KS, Youn HJ, Ryu HS, Chung SS, et al. Osteoconduction at porous hydroxyapatite with various pore configurations. *Biomaterials* 2000;**21**:1291–8.
15. Yoon BH, Park CS, Kim HE, Koh YH. In-situ fabrication of porous hydroxyapatite (HA) scaffolds with dense shells by freezing HA/camphene slurry. *Mater Lett* 2008;**62**:1700–3.
16. Descamps M, Richart O, Hardouin P, Hornez JC, Leriche A. Synthesis of macroporous β-tricalcium phosphate with controlled porous architectural. *Ceram Int* 2008;**34**:1131–7.
17. Descamps M, Duhoo T, Monchau F, Lu J, Hardouin P, Hornez JC, et al. Manufacture of macro-porous β-tricalcium phosphate bioceramics. *J Eur Ceram Soc* 2008;**28**:149–57.
18. Liu DM. Influence of porosity and pore size on the compressive strength of porous hydroxyapatite ceramic. *Ceram Int* 1997;**23**:135–9.
19. Tetsuya T, Takanobu N, Junzo T, Takahiro O, Hideki Y. Novel hydroxyapatite ceramics with an interconnective porous structure exhibit superior osteoconduction in vivo. *J Bio Mater Res* 2002;**59**: 110–7.
20. Lee EJ, Koh YH, Yoon BH, Kim HE, Kim HW. Highly porous hydroxyapatite bioceramics with interconnected pore channels using camphene-based freeze casting. *Mater Lett* 2007;**61**:2270–3.
21. Scheffler M, Colombo P. *Cellular ceramics: structure, manufacturing, properties and applications*. 1st ed. Weinheim: Wiley-VCH; 2005.